Earthquake and tsunami forecasts: Relation of slow slip events to subsequent earthquake rupture

Timothy H. Dixon[a,1], Yan Jiang[b], Rocco Malservisi[a], Robert McCaffrey[c], Nicholas Voss[a], Marino Protti[d], and Victor Gonzalez[d]

[a]School of Geosciences, University of South Florida, Tampa, FL 33620; [b]Pacific Geoscience Centre, Geological Survey of Canada, BC, Canada V8L 4B2; [c]Department of Geology, Portland State University, Portland, OR 97201; and [d]Observatorio Vulcanológico y Sismológico de Costa Rica, Universidad Nacional, Heredia 3000, Costa Rica

Edited* by David T. Sandwell, Scripps Institution of Oceanography, La Jolla, CA, and approved October 24, 2014 (received for review June 30, 2014)

The 5 September 2012 M_w 7.6 earthquake on the Costa Rica subduction plate boundary followed a 62-y interseismic period. High-precision GPS recorded numerous slow slip events (SSEs) in the decade leading up to the earthquake, both up-dip and down-dip of seismic rupture. Deeper SSEs were larger than shallower ones and, if characteristic of the interseismic period, release most locking down-dip of the earthquake, limiting down-dip rupture and earthquake magnitude. Shallower SSEs were smaller, accounting for some but not all interseismic locking. One SSE occurred several months before the earthquake, but changes in Mohr–Coulomb failure stress were probably too small to trigger the earthquake. Because many SSEs have occurred without subsequent rupture, their individual predictive value is limited, but taken together they released a significant amount of accumulated interseismic strain before the earthquake, effectively defining the area of subsequent seismic rupture (rupture did not occur where slow slip was common). Because earthquake magnitude depends on rupture area, this has important implications for earthquake hazard assessment. Specifically, if this behavior is representative of future earthquake cycles and other subduction zones, it implies that monitoring SSEs, including shallow up-dip events that lie offshore, could lead to accurate forecasts of earthquake magnitude and tsunami potential.

earthquake | tsunami | slow slip events | GPS

The great megathrust earthquakes and tsunamis of 2004 (Sumatra) and 2011 (Japan) were reminders that our ability to forecast earthquake magnitude and tsunami risk remains weak. Subduction zone megathrust earthquakes, which tend to be the largest and generate the most destructive tsunamis, are especially problematic because the critical zone of strain accumulation often lies far offshore and is difficult to characterize with on-land sensors. It is also unclear what controls the rupture area, which influences earthquake magnitude, and rupture depth, which influences tsunami potential.

Here we report new analyses of geodetic observations from northwest Costa Rica bearing on these problems. Measurements were made on a peninsula overlying the shallow portion of the megathrust fault, providing sensitivity to seismic loading and release in the critical up-dip (shallow) part of the seismogenic zone. Surface displacements associated with the 5 September 2012 M_w 7.6 Nicoya earthquake (1), as well as preearthquake slow slip events (SSEs) and postearthquake after-slip, were well-recorded. The earthquake did not produce a significant tsunami, even though measurements before the earthquake suggested significant offshore strain accumulation (2). We compare preearthquake strain accumulation to strain release by preearthquake slow slip and coseismic rupture. In contrast to previous studies, we suggest that SSEs have limited predictive value in terms of triggering megathrust earthquakes, at least in this region. However, they do provide critical hazard assessment information by delineating rupture area and the magnitude and tsunami potential of future earthquakes.

Geologic and Seismic Background

The Nicoya Peninsula forms the western edge of the Caribbean plate, where the Cocos plate subducts beneath the Caribbean plate along the Middle American Trench at about 8 cm/y (3). The region has a well-defined earthquake cycle, with large ($M > 7$) earthquakes in 1853, 1900, 1950 (M 7.7), and most recently 5 September 2012 (M_w 7.6). Smaller ($M \sim 7$) events in 1978 and 1990 have also occurred nearby (4). Large tsunamis have not been reported for any of these events (5), but the 1992 M_w 7.6 Nicaragua earthquake 150 km to the northwest generated a large tsunami, reflecting shallow rupture (6, 7). SSEs are common below the Nicoya Peninsula (8, 9). These enigmatic events have now been identified in many subduction zones (10, 11) and represent largely aseismic slip on the plate boundary occurring over weeks or months (12).

Results

Our high-precision GPS network was substantially complete by 2007. We used a special noise minimization technique (9) to define surface displacements from SSEs in this tropical environment (*Methods* and *Supporting Information*). Fig. 1 shows event displacements that are well-recorded (2007 and later). The inter-SSE velocities (average site velocity between the various SSEs, assumed constant over the observation interval) are inverted to estimate coupling (locking) on the plate interface (Fig. 2). The SSE displacements are inverted to estimate slip on the interface during the various events (Fig. 3). We assume that

Significance

Recent destructive megathrust earthquakes and tsunamis in Japan and Sumatra indicate the difficulty of forecasting these events. Geodetic monitoring of the offshore regions of the subduction zones where these events occur has been suggested as a useful tool, but its potential has never been conclusively demonstrated. Here we show that slow slip events, nondestructive events that release energy slowly over weeks or months, are important mechanisms for releasing seismic strain in subduction zones. Better monitoring of these events, especially those offshore, could allow estimates of the size of future earthquakes and their potential for damaging tsunamis. However, the predictive value of slow slip events remains unclear.

Author contributions: T.H.D., M.P., and V.G. designed research; R. McCaffrey contributed new analytic tools; M.P. and V.G. maintained instruments and collected data; T.H.D., Y.J., R. Malservisi, R. McCaffrey, and N.V. analyzed data; and T.H.D., Y.J., R. Malservisi, R. McCaffrey, N.V., M.P., and V.G. wrote the paper.

The authors declare no conflict of interest.

*This Direct Submission article had a prearranged editor.

Freely available online through the PNAS open access option.

Data deposition: All raw data are available at Unavco, the National Science Foundation consortium for geodetic research (www.unavco.org).

[1]To whom correspondence should be addressed. Email: thd@usf.edu.

This article contains supporting information online at www.pnas.org/lookup/suppl/doi:10.1073/pnas.1412299111/-/DCSupplemental.

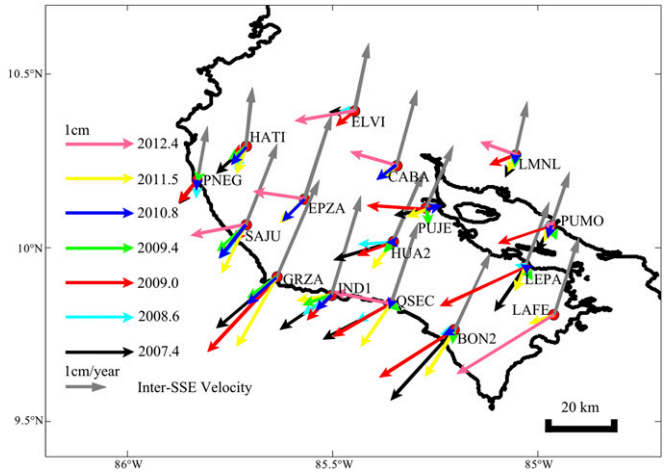

Fig. 1. Surface displacement field for all SSEs recorded in northern Costa Rica since 2007, compared with the average inter-SSE surface velocity field during the same period. Error ellipses are omitted for clarity but are roughly the size of the arrowheads: The mean displacement uncertainty is 0.9 mm and 1.2 mm for the north and east components, respectively, and 0.5 mm/y for both components of velocity (1 SE). Uncertainty estimation procedures are described in ref. 9.

all locking and slip occurs on the fault plane (subduction megathrust), using published slab geometry (13) and inversion techniques (14). The estimated locked or slip patches are 30 km or larger, limited by the spatial resolution of our network (*Supporting Information*).

The temporal resolution of the onset time of individual SSEs is of order 5–10 d, limited by data noise (8, 9). The multiple slip patches shown as single events in Fig. 3 (e.g., 2007.4) probably do not occur simultaneously. They likely migrate both in time and space, but their temporal migration is not well-resolved. Typical migration speeds for SSEs in Cascadia are about 10 km/d (15–17). In Costa Rica, time lags between on-shore events and off-shore events recognized by pressure transients in a borehole hydrologic observatory suggest propagation speeds as high as 20 km/d (18). Because our network only spans about 50 by 100 km, it would take at most 5–10 d for a series of SSEs to migrate across our network, comparable to the temporal resolution of our data. We have therefore considered events together in a single group (a composite event) if they occur within the same 30-d period. Possible up-dip, down-dip, or along-strike migration of several better resolved events is discussed in ref. 9.

The spatial distribution of coseismic rupture for the 2012 earthquake (19) is defined by a dense network of broad-band seismometers, strong motion sensors, and a subset of our GPS stations that recorded dynamic ground displacements at a high rate. These data suggest that the event initiated offshore at ~13 km depth, then ruptured down-dip, reaching a maximum slip of 4.4 m at a depth of about 25 km, stopping at a depth of about 30–35 km near the upper plate Moho. This main rupture patch, beneath the Nicoya Peninsula, is similar to that obtained from static GPS offsets (1). Our inter-SSE locking pattern (Fig. 2) and that obtained from an earlier analysis of campaign and continuous GPS results defining average interseismic site velocities (2) both reveal a locked patch closely coinciding with the 2012 earthquake rupture. However, the new inter-SSE site velocities require an additional locked patch down-dip and east of the 2012 rupture that can be understood in the context of the SSEs that also occur there, as discussed below.

Fig. 3 shows the individual SSEs for 2007 and later and their cumulative slip. The largest events were deeper, down-dip of seismic rupture. However, all recorded events had at least some shallow slip, and four had shallow slip in excess of 30 mm. Shallow SSEs have been reported in only a few subduction zones: New Zealand (20, 21), Japan (22, 23), and Ecuador (24). We suspect the paucity of such events is at least in part a sampling artifact, as many on-shore geodetic networks lack sensitivity to slip events far offshore (25, 26). Our network has sensitivity up to about 30 km offshore, but not beyond (*Supporting Information*). Pressure transients in a borehole hydrologic observatory at the base of the subduction prism offshore the Nicoya Peninsula suggest that some shallow SSEs propagate to within 1 km of the trench (18).

In terms of magnitude and location relative to coseismic rupture, we can distinguish two classes of slow slip:

i) Large events down-dip and mainly east of the main earthquake rupture, in or near the Golfo de Nicoya region, including the one immediately preceding the earthquake (Fig. 3). These events occur near the intersection of the downgoing slab and the upper plate Moho, at the down-dip projection of the Fisher seamount chain.

ii) Smaller offshore events, up-dip of the main earthquake rupture. If slow slip propagates all of the way to the trench, where we lack resolution, the magnitude of up-dip events is underestimated.

When the SSEs in Costa Rica are considered as a group, a striking pattern emerges: They surround the area of coseismic rupture; none occur within the 2012 rupture zone (Figs. 3 and 4). In contrast to the complementary pattern between slow slip and seismic rupture, inter-SSE locking and slow slip have a more complex relationship: Except for a small offshore locked patch to the northwest that is not well-resolved (*Supporting Information*) and the well-resolved earthquake rupture patch, many locked regions also slip in SSEs (Figs. 2 and 4). The summed moment for the 2007 and later SSEs (1.6×10^{20} Nm) is equivalent to an M 7.5 earthquake, suggesting that SSEs constitute an important part of the strain release budget.

If the rate and spatial pattern of strain accumulation were constant over the entire 62-y (1950–2012) interseismic period, a fully locked patch would have a total slip deficit of about 5 m. The maximum coseismic slip in 2012 was comparable (4.4 m); a M_w 6.9 event in 1978 (1, 19) may have contributed to the small

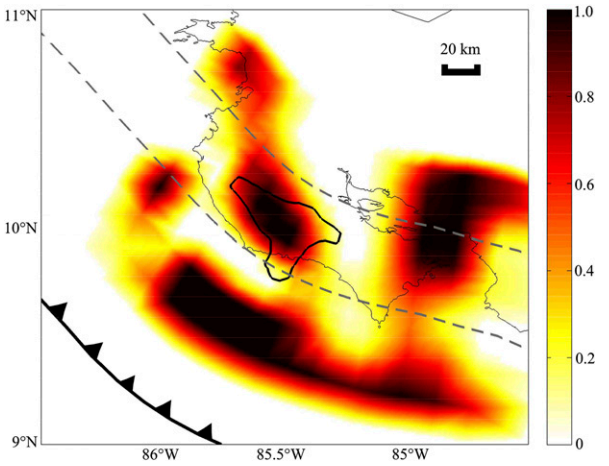

Fig. 2. Amount of locking (1, fully locked; 0, slipping) on the plate interface associated with the inter-SSE velocity field shown in Fig. 1. Heavy line with teeth (on upper plate, pointing in the down-dip direction) shows the location of the Middle America Trench. Dashed lines represent depth contours on the dipping plate interface, at 20 km and 45 km, respectively (13). The rupture area of the 2012 earthquake (19) is outlined with a black line (see also Fig. 4) coinciding with a preearthquake locked patch.

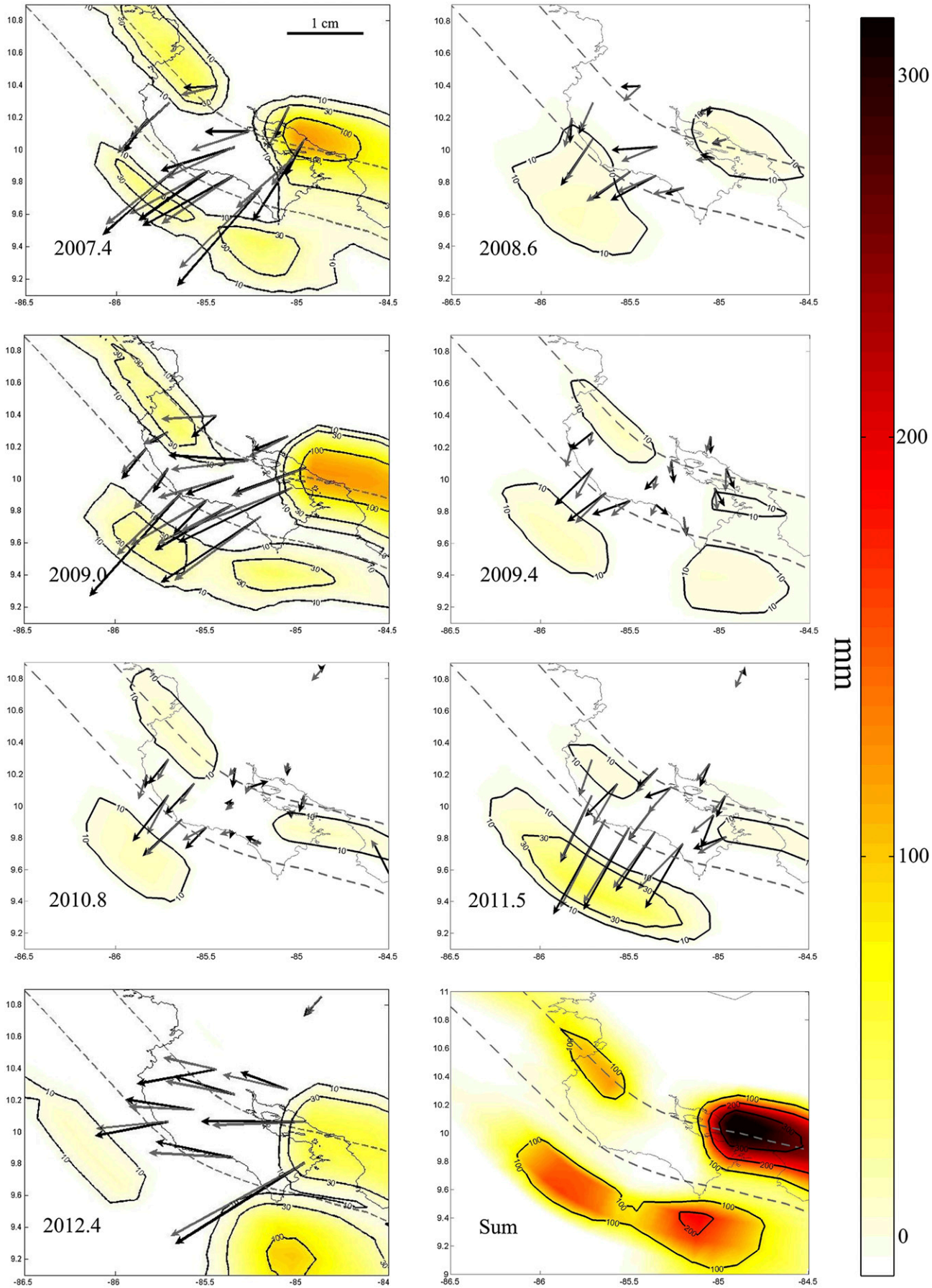

Fig. 3. Slip (mm) on the plate interface associated with individual SSEs shown in Fig. 1. *Bottom Right* panel shows summed slip for the period 2007–2012. Dashed lines represent depth contours on the plate interface, at 20 and 45 km, respectively.

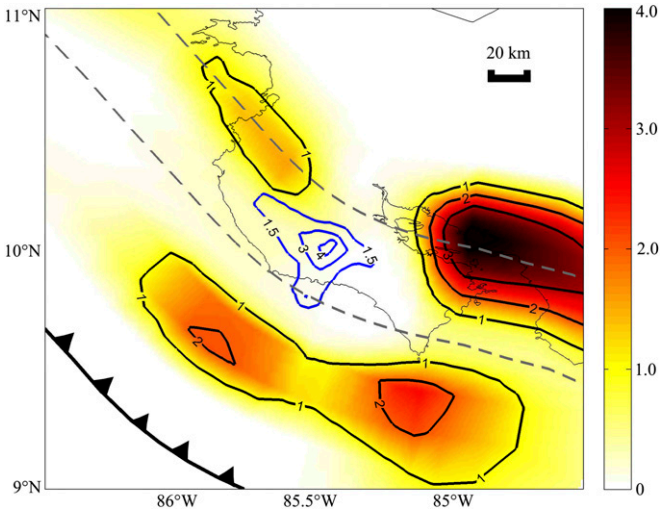

Fig. 4. Summed SSE slip on the plate interface (black contours in meters, yellow, orange, and red colors) for the entire (1950–2012) interseismic period, assuming the 2007–2012 measurement period is typical. For comparison, the patch that ruptured in the 2012 earthquake (19) is also shown (in center, blue contours in meters).

difference. We can compare the amount of released and deficit slip to summed slow slip from the various SSE patches if we similarly assume that the rate and spatial pattern of slow slip over the interseismic period were constant and adequately sampled by the 2007–2012 data (Fig. 4). With these assumptions, down-dip SSEs released up to 4 m of slip, close to the amount expected. The down-dip slow slip patch was thus able to limit the rupture size of the 2012 event by intermittent release of strain in a series of large SSEs, roughly every 2–3 y if the post-2007 record is typical. In contrast, up-dip SSEs summed to no more than a 2-m slip, a little less than half the expected amount (postseismic slip will presumably account for an additional fraction). If the modern rate of SSEs has been constant since the last earthquake in 1950, the summed moment for all of the SSEs over this period (2×10^{21} Nm) is nearly an order of magnitude higher than the moment released by the 2012 earthquake (3.5×10^{20} Nm) and is equivalent to a M_w 8.2 earthquake. SSEs thus appear to be releasing 80–90% of the slip associated with relative plate motion, consistent with the historically low seismic coupling coefficient for this margin (27–29). We suggest that Central America tends to have smaller earthquakes compared with many other subduction zones because a significant fraction of slip occurs via frequent SSEs. Of course, we do not know if such behavior will continue in the future. Prior events in 1900 and 1950 appear to have ruptured approximately the same patch (1, 19). The better located 1978 event (Mw 6.9) was smaller than the 2012 event (Mw 7.6) but also ruptured in the same area.

Discussion

Since episodic tremor and SSEs were first identified in the Cascadia subduction zone (30), it has been assumed that slow slip would "load" the seismogenic zone, bringing it closer to failure and possibly triggering a major earthquake (15, 31–33). In Japan, foreshocks and a series of repeating earthquakes several weeks before the 2011 Tohoku earthquake migrated toward the hypocenter, leading to speculation that shallow slow slip triggered the rupture: "If this kind of premonitory slow slip behavior also precedes other large earthquakes, [it will] have crucial implications for earthquake prediction and risk assessment" (33).

One difficulty in assessing the argument that slow slip triggered the 2011 Tohoku earthquake is that the on-shore GPS network was too far away to record shallow SSEs. SSEs were inferred largely on the basis of seismicity (33). Our studies suggest that shallow SSEs do not always colocate with seismic tremor or low-frequency earthquakes (8); hence, seismicity alone may not be diagnostic. Limited available geodetic data are far from definitive, although they have been interpreted to support the triggering hypothesis for the 2011 Tohoku earthquake (34). SSEs in other subduction zones have also been interpreted to support the triggering hypothesis (35, 36). Our data describe, to our knowledge, the first well-recorded shallow SSEs in the decade leading up to a large subduction zone earthquake and a deeper event in 2012 immediately before the earthquake (*Supporting Information*), allowing a rigorous examination of the triggering hypothesis. Unfortunately, the predictive value of such events remains unclear. Two observations are relevant:

i) Broadly similar SSEs in 2007 and 2009 did not trigger a major plate interface earthquake (smaller within-plate earthquakes occurred near the time of some SSEs, but whether these were triggered or coincidental is not clear).

ii) Changes in Mohr–Coulomb failure stress (ΔCFS) (37, 38) associated with the 2012 SSE using the same plate interface geometry (13) show somewhat elevated (up to ∼0.5 bars) ΔCFS near the down-dip end of the earthquake rupture (*Supporting Information*). However, this was not where the rupture initiated; rather, it initiated offshore, then propagated down-dip (19). ΔCFS at this up-dip location was less than 0.2 bars, below thresholds commonly assumed in these calculations. In subduction environments, ΔCFS ∼1–25 bars have been shown to influence aftershock location and promote subsequent large thrust earthquakes (39). Using all of the SSEs since 2007 gives ΔCFS values of ∼0.3–0.6 bars at the nucleation point, closer but still below the accepted triggering threshold. Poro-elastic processes are not considered in such calculations and could contribute to overall stress change (40). We also cannot preclude a cascade effect not directly related to stress triggering, whereby slow slip initiates a process that evolves into an earthquake (41).

SSEs can be described in terms of a conceptually simple rate-state friction model, consistent with a range of faulting behavior including earthquakes and after-slips (42–47). In this model, earthquake rupture occurs on locked patches of the plate interface that have accumulated significant stress and are velocity-weakening (friction decreases as slip velocity increases), whereas slow slip and after-slip occur on patches that are perhaps at lower stress and are velocity-strengthening (friction increases as slip velocity increases). Patches with near-neutral frictional characteristics are conditionally stable and may behave in either mode depending on stress or other physical conditions. Our results are broadly consistent with this view: Areas of the plate interface subject to frequent SSEs did not rupture in the main earthquake, consistent with velocity-strengthening behavior. We suggest this occurs for at least two different reasons, reflecting the two different classes of SSEs that we observe: their different pressure, temperature, and compositional (e.g., water content) environments, and presumably different types of velocity-strengthening behavior.

Down-dip of the main coseismic rupture, relatively large SSEs relieved all or most slip deficits during the interseismic period. SSEs in the same depth range have been reported in Alaska (48), Cascadia (49), and Japan (11, 50), perhaps highlighting frictional conditions that also contribute to deep after-slip in subduction zones (51) and similarly help to define the extent of subsequent coseismic rupture (49).

Up-dip of the main rupture, SSEs did not release all accumulated slip deficits; nevertheless, rupture propagation stopped close to the coastline and did not continue into the offshore

locked patch. Either some strain is transmitted to the next seismic cycle (52), or it will be released as after-slip in the near future. Preliminary observations suggest that significant offshore after-slip is occurring, but it will be several more years before an accurate strain release budget can be calculated.

The large contrasts in pressure, temperature, and pore fluid pressure that characterize ambient conditions for shallow versus deep slow slip suggest that different physical processes are responsible for the two classes of events. Large variations in pore fluid pressure are more likely in the shallow region (sediments are largely dewatered by the time they reach the depth of deep slow slip), and these variations can have a significant impact on frictional conditions and resolved normal stress. Regardless of process, shallow SSEs limit tsunami potential in at least one and possibly two ways: by releasing some accumulated slip deficit and perhaps by marking frictional properties that limit seismic rupture. Of course, frictional properties can change over time. As an example, after-slip, usually considered an indicator of velocity-strengthening behavior, has been observed in areas that had previously undergone seismic (velocity-weakening) behavior (53). Understanding why such changes occur is an important research topic.

In contrast to previous studies, our results do not support the idea that SSEs have predictive value for the timing of megathrust earthquakes, at least with current data and model limitations. However, our findings do suggest that SSEs provide important constraints for earthquake magnitude and tsunami forecasting: SSEs limited the size of the 2012 earthquake by releasing a large fraction of the interseismic strain and revealed regions of velocity-strengthening that may have limited rupture propagation, especially offshore, limiting the subsequent tsunami. Better monitoring and understanding of these events could therefore improve hazard forecast accuracy, especially if future studies show that our results are broadly applicable to other subduction zones.

Current technology is not well-suited to the precise, spatially dense, and high time-resolution monitoring that is required to detect shallow SSEs in typical subduction zones (54), where geography limits geodetic resolution in the critical offshore region. For example, sea floor pressure gauges provide good temporal sampling, but are subject to drift and spurious signals from transient oceanographic events and are also expensive to deploy in sufficient numbers for good spatial sampling. Development of improved techniques for sea floor geodesy is urgently needed.

Methods

GPS data analysis and uncertainty estimation follow ref. 9. Briefly, the phase and pseudorange data are recorded at 15-s intervals and decimated to 5-min samples. Nine stations also record data at 5 Hz for strong ground motion studies (8, 19). A complete description of network hardware is given in ref. 8. The decimated data are used to estimate 24-h average position estimates of the receiver antenna phase center, assumed to be fixed relative to the ground via large monuments. Noise minimization includes identification and removal of annual terms reflecting atmospheric and hydrological effects and regional filtering to identify and remove common-mode errors, likely related to satellite orbit and reference frame effects. The resulting position time series define surface displacements associated with SSEs as well as long-term site velocities associated with the locked plate interface. The estimated displacements are used as inputs to a dislocation model (14) to estimate slip on the plate interface during a SSE. The estimated plate interface displacements are then used as inputs into Coulomb 3.3 (38), a model for estimating changes in ΔCFS on a fault associated with nearby displacements. Detailed descriptions of the data analysis, dislocation modeling and inversions for slip at depth, and the ΔCFS analysis are given in *Supporting Information*.

ACKNOWLEDGMENTS. We thank two anonymous reviewers, whose comments greatly improved the manuscript. We thank Unavco for assistance with installing and maintaining the GPS network in the Nicoya Peninsula. This work was supported by National Science Foundation Grants OCE-0841091 and 1158167 and EAR-0842137, 1140261, and 1345100 from the Margins, Tectonics, Instrumentation-Facilities, and Geophysics programs (to T.H.D.). Y.J. was supported by a NASA Earth and Space Science Fellowship.

1. Protti M, et al. (2014) Nicoya earthquake rupture anticipated by GPS measurements of the locked plate interface. *Nat Geosci* 7:117–121.
2. Feng L, et al. (2012) Active deformation near the Nicoya Peninsula, northwestern Costa Rica, between 1996 and 2010: Interseismic megathrust coupling. *J Geophys Res* 117, 10.1029/2012JB009230.
3. DeMets C (2001) A new estimate for present day Cocos & Caribbean Plate motion: Implications for slip along the Central American Volcanic Arc. *Geophys Res Lett* 28: 4043–4046.
4. Protti M, et al. (1995) The March 25, 1990(Mw = 7.0, ML = 6.8), earthquake at the entrance of the Nicoya Gulf, Costa Rica: Its prior activity, foreshocks, aftershocks, and triggered seismicity. *J Geophys Res* 100:20,345–20,358.
5. Chacón-Barrantes SE, Protti M (2011) Modeling a tsunami from the Nicoya, Costa Rica, seismic gap and its potential impact in Puntarenas. *J S Am Earth Sci* 31:372–382.
6. Satake K (1994) Mechanism of the 1992 Nicaragua tsunami earthquake. *Geophys Res Lett* 21:2519–2522.
7. Kikuchi M, Kanamori H (1995) Source characteristics of the 1992 Nicaragua tsunami earthquake inferred from teleseismic body waves. *Pure Appl Geophys* 144:441–453.
8. Outerbridge KC, et al. (2010) A tremor and slip event on the Cocos-Caribbean subduction zone as measured by a global positioning system (GPS) and seismic network on the Nicoya Peninsula, Costa Rica. *J Geophys Res* 115:B10408.
9. Jiang Y, et al. (2012) Slow slip events in Costa Rica detected by continuous GPS observations, 2002-2011. *Geochem Geophys Geosyst* 13:Q04006.
10. Schwartz SY, Rokosky JM (2007) Slow slip events and seismic tremor at circum-Pacific subduction zones. *Rev Geophys* 45:RG3004.
11. Beroza GC, Ide S (2011) Slow earthquakes and nonvolcanic tremor. *Annu Rev Earth Planet Sci* 39:271–296.
12. Brodsky EE, Mori J (2007) Creep events slip less than ordinary earthquakes. *Geophys Res Lett* 34:L16309.
13. Hayes GP, Wald DJ, Johnson RL (2012) Slab1.0: A three-dimensional model of global subduction zone geometries. *J Geophys Res* 117:B01302.
14. McCaffrey R (2009) Time dependent inversion of three component continuous GPS for steady and transient sources in northern Cascadia. *Geophys Res Lett* 36:L07304.
15. Rogers G, Dragert H (2003) Episodic tremor and slip on the Cascadia subduction zone: The chatter of silent slip. *Science* 300(5627):1942–1943.
16. McCausland WA, Creager KC, Rocca ML, Malone SD (2010) Short-term and long-term tremor migration patterns of the Cascadia 2004 tremor and slow slip episode using small aperture seismic arrays. *J Geophys Res* 115:B00A24.
17. Vidale JE, Houston H (2012) Slow slip: A new kind of earthquake. *Phys Today* 65(1): 38–43.
18. Davis EE, Villinger H, Sun T (2014) Slow and delayed deformation and uplift of the outermost subduction prism following ETS and seismogenic slip events beneath Nicoya Peninsula, Costa Rica. *Earth Planet Sci Lett*, in press.
19. Yue H, et al. (2013) The 5 September 2012 Costa Rica M_w 7.6 earthquake rupture process from joint inversion of high-rate GPS, strong-motion, and teleseismic P wave data and its relationship to adjacent plate boundary interface properties. *J Geophys Res* 118:5453–5466.
20. Douglas A, Beavan J, Wallace L, Townend J (2005) Slow slip on the northern Hikurangi subduction interface, New Zealand. *Geophys Res Lett* 32:L16305.
21. Wallace LM, Beavan J (2010) Diverse slow slip behavior at the Hikurangi subduction margin, New Zealand. *J Geophys Res* 115(B12):B12402.
22. Sagiya T (2004) Interplate coupling in the Kanto district, central Japan, and the Boso Peninsula silent earthquake in May 1996. *Pure Appl Geophys* 161:2327–2342.
23. Ozawa S, Suito H, Tobita M (2007) Occurrence of quasi-periodic slow slip off the east coast of the Boso Peninsula, central Japan. *Earth Planets Space* 59:1241–1245.
24. Vallee M, et al. (2013) Intense interface seismicity triggered by a shallow slow slip event in the Central Ecuador subduction zone. *J Geophys Res* 118:2965–2981.
25. Wang K, Dixon TH (2004) Coupling semantics and science in earthquake research. *EOS* 85(18):180–181.
26. LaFemina P, et al. (2009) Fore-arc motion and Cocos Ridge collision in Central America. *Geochem Geophys Geosys* 10:Q05S14.
27. McNally KC, Minster JB (1981) Nonuniform seismic slip rates along the Middle America Trench. *J Geophys Res* 86(B6):4949–4959.
28. Pacheco JV, Sykes LR, Scholz CH (1993) Nature of seismic coupling along simple plate boundaries of the subduction type. *J Geophys Res* 98:14,133–14,159.
29. Scholz CH, Campos J (2012) The seismic coupling of subduction zones revisited. *J Geophys Res* 117:B05310.
30. Dragert H, Wang K, James TS (2001) A silent slip event on the deeper Cascadia subduction interface. *Science* 292(5521):1525–1528.
31. Mazzotti S, Adams J (2004) Variability of near-term probability for the next great earthquake on the Cascadia subduction zone. *Bull Seismol Soc Am* 94:1954–1959.
32. Miyazaki S, McGuire JJ, Segall P (2011) Seismic and aseismic fault slip before and during the 2011 off the Pacific coast of Tohoku earthquake. *Earth Planets Space* 63: 637–642.
33. Kato A, et al. (2012) Propagation of slow slip leading up to the 2011 M(w) 9.0 Tohoku-Oki earthquake. *Science* 335(6069):705–708.
34. Ito Y, et al. (2013) Episodic slow slip events in the Japan subduction zone before the 2011Tohoku-Oki earthquake. *Tectonophys* 600:14–26.

35. Graham, et al. (2014) GPS constraints on the 2011–2012 Oaxaca slow slip event that preceded the 2012 March 20 Ometepec earthquake, southern Mexico. *Geophys J Int* 197:1593–1607.
36. Ruiz, et al. (2014) Intense foreshocks and a slow slip event preceded the 2014 Iquique Mw 8.1 Earthquake. *Science* 345:1165–1169.
37. Stein RS, Barka AA, Dieterich JH (1997) Progressive failure on the North Anatolian fault since 1939 by earthquake stress triggering. *Geophys J Int* 128:594–604.
38. Toda S, Stein RS, Sevilgen V, Lin J (2011) *Coulomb 3.3 Graphic-Rich Deformation and Stress-Change Software for Earthquake, Tectonic, and Volcano Research and Teaching—User Guide* (U.S. Geological Survey Open-File Report), Vol 2011–1060, 63 pp.
39. Lin J, Stein RS (2004) Stress triggering in thrust and subduction earthquakes and stress interaction between the southern San Andreas and nearby thrust and strike-slip faults. *J Geophys Res* 109, 10.1029/2003JB002607.
40. Davis E, Heesemann M, Wang K (2011) Evidence for episodic aseismic slip across the subduction seismogenic zone off Costa Rica: CORK borehole pressure observations at the subduction prism toe. *Earth Planet Sci Lett* 306:299–305.
41. Segall P, Bradley AM (2012) Slow-slip evolves into megathrust earthquakes in 2D numerical simulations. *Geophys Res Lett* 39:L18308.
42. Dieterich JH (1992) Earthquake nucleation on faults with rate and state-dependent friction. *Tectonophys* 211:115–134.
43. Marone CJ (1998) Laboratory-derived friction laws and their application to seismic faulting. *Annu Rev Earth Planet Sci* 26:643–696.
44. Liu Y, Rice JR (2005) Aseismic slip transients emerge spontaneously in three-dimensional rate and state modeling of subduction earthquake sequences. *J Geophys Res* 110:B08307.
45. Johnson KM, Bürgmann R, Larson K (2006) Frictional properties on the San Andreas fault near Parkfield, California, inferred from models of afterslip following the 2004 earthquake. *Bull Seismol Soc Am* 96:S-321–S-338.
46. Hsu YJ, et al. (2006) Frictional afterslip following the 2005 Nias-Simeulue earthquake, Sumatra. *Science* 312(5782):1921–1926.
47. Barbot S, Lapusta N, Avouac J-P (2012) Under the hood of the earthquake machine: Toward predictive modeling of the seismic cycle. *Science* 336(6082): 707–710.
48. Ohta Y, Freymueller JT, Hreinsdotir S, Suito H (2006) A large slow slip event and the depth of the seismogenic zone in the south central Alaska subduction zone. *Earth Planet Sci Lett* 247:108–116.
49. Chapman JS, Melbourne TI (2009) Future Cascadia megathrust rupture delineated by episodic tremor and slip. *Geophys Res Lett* 36:L22301.
50. Peng Z, Gomberg J (2010) An integrated perspective of the continuum between earthquakes and slow-slip phenomena. *Nat Geosci* 3:599–607.
51. Perfettini H, Avouac J-P, Ruegg J-C (2005) Geodetic displacements and aftershocks following the 2001 Mw = 8.4 Peru earthquake: Implications for the mechanics of the earthquake cycle along subduction zones. *J Geophys Res* 110:B09404.
52. Goldfinger C, Ikeda Y, Yeats RS, Ren J (2013) Superquakes and supercycles. *Seismol Res Lett* 84:24–32.
53. Johnson KM, Fukuda J, Segall P (2012) Challenging the rate-state asperity model: Afterslip following the 2011 M9 Tohoku-oki, Japan, earthquake. *Geophys Res Lett* 39, 10.1029/2012GL052901.
54. Newman AV (2011) Hidden depths. *Nature* 474(7352):441–443.